Analysis on the Causative Fault of the 2021 Mw 6.0 Tehoru Earthquake in the South Coast of Seram Island: A Preliminary Result

Gatut Daniarsyad[1*], *Priyobudi* Priyobudi[1], *Aprilia* Puspita Cahyaningrum[1], *Dayu* Gigih Wibisono[1], *Sesar* Prabu Dwi Sriyanto[1], *Abdul* Rosid[1], *Bayu* Pranata[1], *Indra* Gunawan[1], *Iman* Fatchurochman[1] and *Daryono* Daryono[1]

[1]Agency for Meteorology Climatology and Geophysics of Indonesia, Jakarta, Indonesia

Abstract. Seram Island is the northern part of the Banda subduction which is characterized by the existence of a thrust fault structure in the Seram Trough as the main contributor to seismicity in this region. Complex tectonic activity also forms a deformation zone of the Kawa Fault with a sinistral strike slip mechanism and high-angle normal faults in the mainland. On June 16, 2021 a Mw 6.0 earthquake occurred on the south coast of Seram, in Tehoru to be precise, which followed by a small tsunami wave which is thought to have been generated by an underwater landslide. This earthquake has a normal fault mechanism which is quite rare on Seram Island, however, the actual fault plane that caused the earthquake is still unknown. In this study, we investigate potential faults that may have caused the 2021 Tehoru earthquake by performing a seismicity analysis using well relocated hypocenter of the mainshock and the aftershocks sequence. We use the double-difference relocation method with the SVD algorithm performed in the hypoDD program. The results show the distribution of aftershocks that form a northeast-southwest trending lineation. The depth of the hypocenter has also improved from being dominated by fixed depth to being varied with dominance at depths of 8-14 km. An important feature of the relocation results is that the aftershocks distributed downward along a ~35° northwest-dipping plane which indicates a southwest-northeast fault orientation. This result confirmed by using geodetic observations that shows a horizontal displacement of 14 mm toward northwest direction and a land subsidence of 14 mm. This southwest-northeast oriented fault structure is thought to be associated with high-angle normal fault resulting from a north-south extension activity in the central part of Seram Island. The results of this study indicate the existence of other local fault structure in the Seram Island which can be used as a basis for seismic hazard assessment, other than seismic activities from Seram Trough and Kawa Fault.

1 Introduction

On Wednesday, 16 June 2021, at 13:43 local time (Eastern Indonesia Time), the Maluku region, Indonesia, was hit by a tectonic earthquake. The earthquake epicenter is located on the southern coast of Seram Island at coordinates 3.42°S and 129.57°E, or precisely in the coastal area of Tehoru subdistrict, Central Maluku Regency, Maluku Province, at a depth of 11 km (Figure 1). Indonesian Agency for Meteorology Climatology and Geophysics (BMKG) obtained an updated magnitude of Mw 6.0 with the normal-fault mechanism from seismic waveform analysis. It is thought to be caused by a previously unmapped local fault activity. This earthquake was felt by community up to IV MMI (Modified Mercalli Intensity) scale in numerous areas, namely Tehoru, Masohi, Bula, Kairatu, Saparua, and Wahai. The shaking reaches III MMI scale in Ambon City, the capital of Maluku Province. Based on information from National Disaster Management Authority (BNPB), there were more than 50 damaged residential buildings in Saunolu and Mahu Village, with no fatalities due to this earthquake.

A small-scale tsunami also occurred after the 2021 Tehoru earthquake. A tsunami with a maximum height of up to 51 cm was recorded at the Tehoru tide gauge station 2 minutes after the earthquake's origin time [1]. Tsunamis with a maximum height of 2 cm and 3.4 cm were also recorded at the Amahai (14 minutes) and Banda (18 minutes) tide gauge stations, respectively. [1] explained that the tsunami was generated by a combination of submarine deformation due to earthquake and landslide. The tsunami numerical model with only an earthquake source has not been able to reconstruct a comparable observed tsunami waveform at the Tehoru station. This high-frequency waveform is possibly generated by submarine landslides with a length and thickness of 4 km and 50 m, respectively [1]. The local community has to be cautious with a strong earthquake since it potentially causes damage to infrastructure and possibly triggers underwater landslides that generate a tsunami.

Focal mechanism analysis from BMKG shows that the earthquake has a normal faulting mechanism with

*Corresponding author: lp.daniarsyad@gmail.com

two nodal planes that have parameter of strike 252°, dip 39°, and rake -38° for first nodal plane and strike 13°, dip 67°, and rake -122° for second nodal plane. However, we cannot determine the actual fault plane from those two available nodal planes because no information on active faults that has been mapped in this region. The distribution of the main shock and its aftershocks until 30 July 2021 from BMKG monitoring (Figure 1) appears to be spreading in the Tehoru subdistrict area and around the Teluti Bay, with a dominant distribution trending southwest-northeast. It is difficult to interpret the causative fault of this event since the main deformation zone on Seram Island is described has a northwest-southeast orientation [2]. Therefore, in this study, we aim to investigate the fault that was responsible for the 2021 Tehoru earthquake. It is necessary to have a reliable location on the aftershock sequence as well as the mainshock to give a better explanation on the causative fault and the fault structures in the region. Here we perform hypocenter relocation to obtain the more precise mainshock and aftershock hypocenter location. The results of the earthquake relocation are expected to be able to explain the geological structure that caused the 2021 Tehoru earthquake.

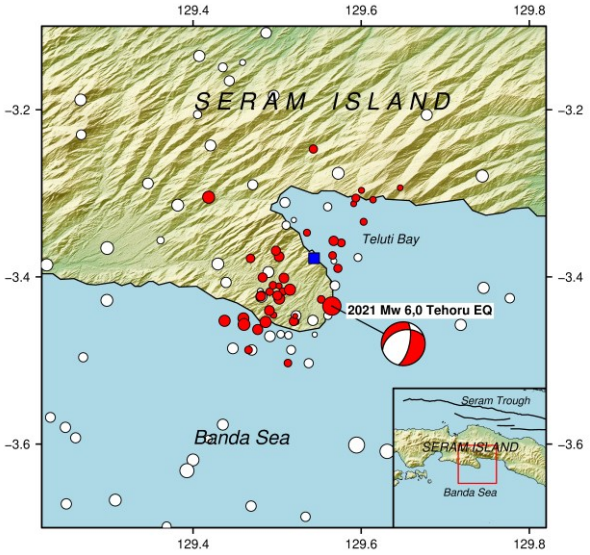

Fig. 1. Map showing the mainshock and the aftershock of the 2021 Tehoru earthquake (red circles) and background seismicity from 2009 to 2021 (white circles) from BMKG catalog. Blue square denotes the Tehoru subdistrict center.

2 Tectonic structure

Seram Island is located in the northern part of the Banda Arc. This region is categorized as a subduction structure, as indicated by the presence of thrust faults and the Seram Trough. The Seram Trough is a subsided deformation front due to loading caused by the development of belt-folding masses and reverses faults [3]. In addition, horizontal fault structures also occur in the Banda Arc. The Kawa Fault is one of the significant structure in the northern Banda Arc. The Kawa Fault originates from a low-angle detachment fault which is currently turning into a left lateral fault [2,4]. A sinistral fault also exists off the east coast of Seram [5,3). The Kawa and offshore strike-slip fault form a shear zone called the Kawa-Kumawa Shear Zone [6]. It has been active since the Jurassic period and reactivated during subduction rollback.

The central part of Seram is a mountainous area with a maximum elevation of 3000 m on Mount Manusela. Two active fault structures, namely the Kawa and Manusela faults, have been identified. The active fault traces typically cut across the mountainous region of Seram in a northwest-southeast direction. The ~137 km long Kawa Fault crosses mountainous terrain from north of Elpaputih Bay to north of Teluti Bay (Figure 2). The Kawa Fault is divided into four geometric segments, from east to west: the Teluti, Alau, Nakupia, and Mala segments. The Teluti segment diverges into two subsegments in the Teluti Valley, namely the northern and southern sections [7]. The northern part is still a sinistral fault, while the southern one is a normal fault where the Teluti Valley is the footwall. The southern segment is nearby the epicenter of the Tehoru earthquake.

Deformation on Seram Island, including the Kawa shear zone, fold-thrust belt, and Seram Trough, is caused by oblique convergent strike-slip tectonic (transpression). This is demonstrated by sandbox modeling where the Sorong Fault and Tarera-Aiduna Fault act as boundary strike-slip faults in the north and south of Seram Island [8]. Then an opposite shear force is applied so that deformation occurs around Seram Island. Within the deformation zone there are shear, pressure and tension forces at the same time. Figure 2 shows the geological structures that develop on Seram Island which is devided as shear zones, fault detachment, and high-angle normal faulting [4].

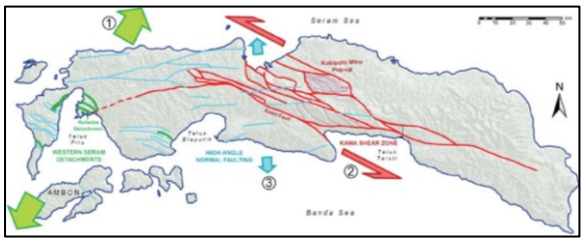

Fig. 2. Schematic diagram of geological structure in Seram Island showing the western Seram detachment faults (green), strike-slip faults in Kawa shear zone (red), and high-angle normal faults (blue) [4].

3 Data and methods

In this study, hypocenter relocation is carried out for the 2021 Tehoru earthquake sequence from the mainshock and its aftershocks. The data used is P and S wave arrival time catalog from BMKG seismic network for the time period of 16 June until 30 July 2021 with area boundaries from 3.10°S–3.70°S and 129.20°E–129.80°E. Based on that period and area boundaries, 40 earthquakes were obtained with a total of 391 P-wave phase arrival times and 63 S-wave phase arrival times recorded at 24 seismic stations (Figure 3). The stations distribution shows fairly good coverage of the study area, except in the southwest direction towards the Banda Sea where there are no stations nearby.

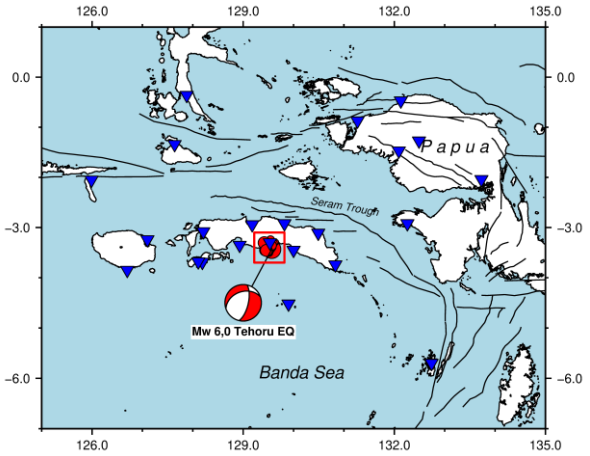

Fig. 3. Distribution of stations used in relocation denoted by blue-colored inverted triangles. Study area indicated by red square.

This study uses the double-difference relocation method [9] which is performed using the hypoDD program [10]. This method has been successfully used to explain newly identified fault in Indonesia e.g., the 2017 Mw 6.6 Poso earthquake [11] and the 2019 Mw 6.5 Ambon earthquake [12], as well as describing significant tectonic feature [13]. The hypoDD requires differential travel time data for each pair of earthquakes at the same station, which can be derived from catalog data or cross-correlation data.

In this study, differential travel time data is generated only from BMKG arrival time catalog data using ph2dt program based on several parameters. The maximum distance between earthquake pairs and the station is limited to 500 km with the maximum distance between hypocenters is 30 km. The minimum observation used is 4 phases considering that the station distribution is not too close and the earthquake magnitude is relatively small, while the maximum number of observations is 24 phases or as many as the number of stations. Based on the parameters above, 476 pairs of earthquakes were obtained with 3001 pairs of P-phase travel times and 303 pairs of S-phase travel times. The farthest hypocenter distance between pairs of earthquakes is 25.76 km, with the average hypocenter distance for strongly linked earthquakes is 9.27 km. This differential travel time data is then used in relocating the hypocenter using the hypoDD program.

The 6-layer velocity model structure (Table 1) is used in relocating the hypocenter of the 2021 Tehoru earthquake sequence which is a combination of the 1D velocity model from local network in western Seram [12] and the AK135 global velocity model [14]. The Vp/Vs of 1.75 is used in the relocation which is obtained from the Wadati diagram based on travel time data from the aftershocks sequence. Hypocenter relocation is carried out using a singular value decomposition (SVD) algorithm which is efficiently used for a series of earthquakes in a small system and can demonstrate the reliability of relocation results through least squares errors [9,10].

Table 1. Velocity model used in the relocation.

Top of layer (km)	P-wave velocity (km/s)
0	5,00
8,5	5,20
16,5	6,25
24	6,90
29	8,00
80	8,09

4 Result and discussion

In general, the improvement in the hypocenter location from the relocation result can be seen through the distribution of residual travel time (Figure 4). The figure shows a comparison of the distribution of travel time residuals before and after relocation where before relocation there are still travel time residuals of more than ± 3 seconds with small residuals (close to zero) not until 200 data. Whereas the residual after relocation with value more than ± 3 seconds does not reach 1% and only 10% of the data has a residual of more than ± 1 second. The amount of data that is close to zero is also increasing after the relocation, which is more than 350 data.

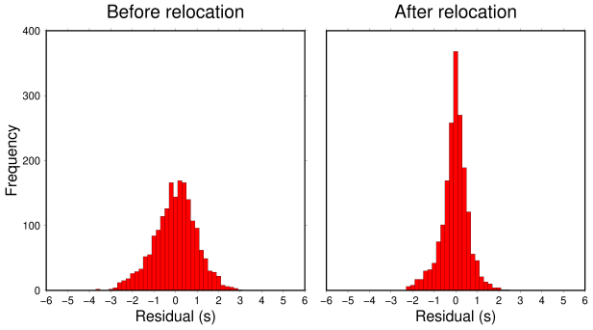

Fig. 4. Comparison of the travel time residual before relocation (left) and after relocation (right).

A total of 19 earthquakes were successfully relocated with an average epicenter displacement of 3.25 km where the farthest epicenter shift reached 8.76 km and the closest shift was 0.97 km. This small displacement indicates that the location of the epicenter from the BMKG data is quite good. The map of epicenters shifting (Figure 5) shows a more clustered epicenters distribution after the relocation. The direction of the shift of the epicenter varies, dominated by a shift in the east-west direction which shows that the epicenters of the earthquake are getting closer to a northeast-southwest oriented lineation.

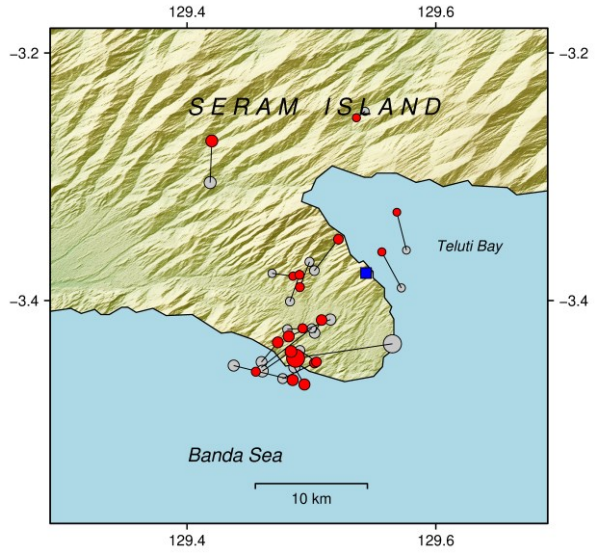

Fig. 5. Epicenter location shift map with epicenter before relocation (gray circles) and after relocation (red circles) are connected by black line.

Meanwhile, in the earthquake depth parameter, there is an average change of 2.20 km with the farthest depth change is 5.45 km and the closest is 0.50 km. Although the depth of the hypocenter also did not experience a large shift, the relocation results made a significant change because only 2 of the 19 earthquakes in the BMKG data had non-fixed depth (Figure 6). After being relocated, the depth of the earthquake hypocenter became more varied from the shallowest of 4.55 km to the deepest of 16.94 km (Figure 7). Most of the earthquakes are distributed at depths of 8–14 km with a total of 15 earthquakes or almost 80% of the total data. A significant change in the location of the epicenter occurred in the main earthquake of Mw 6.0. The epicenter of the main earthquake which was previously located in the western coastal area shifted more than 8 km to the east and converged with most of the aftershock activity. The depth of the hypocenter of the main earthquake which was initially 11.2 km became shallower to 9.14 km.

Other parameter in assessing the quality of relocation results with the SVD algorithm are using horizontal and vertical errors which indicate the uncertainty of the hypocenter location. Figure 7 shows the distribution of relocated epicenters and hypocenters with error bar lines for each earthquake. The average error on longitude is about 760 meters and average latitude error is about 1.1 km. Meanwhile, the average vertical error or depth is less than 1 km (946.4 meters). There were two earthquakes located northward from the main cluster with uncertainty more than 1.5 km which may be caused by the large distance from the main cluster, however, the RMS (root mean square) value of these two earthquakes is still less than 1. This shows that the quality of the hypocenter relocation result of the 2021 Tehoru earthquake sequence is quite good mathematically.

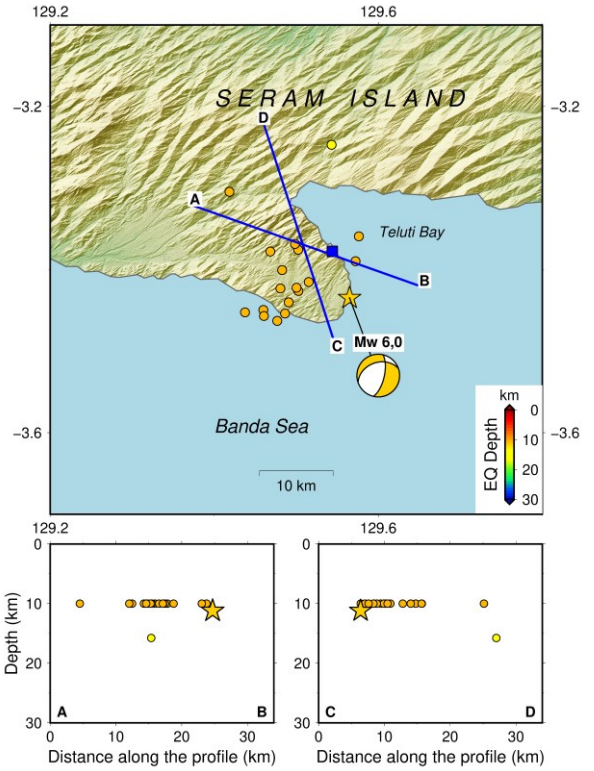

Fig. 6. Hypocenter distribution and vertical section before relocation for the mainshock (star) and the aftershocks (circles). Earthquakes depth is indicated by the color scale. Blue lines denote the cross-section profile perpendicular to the strike 13° fault plane (A-B) and strike 252° fault plane (C-D).

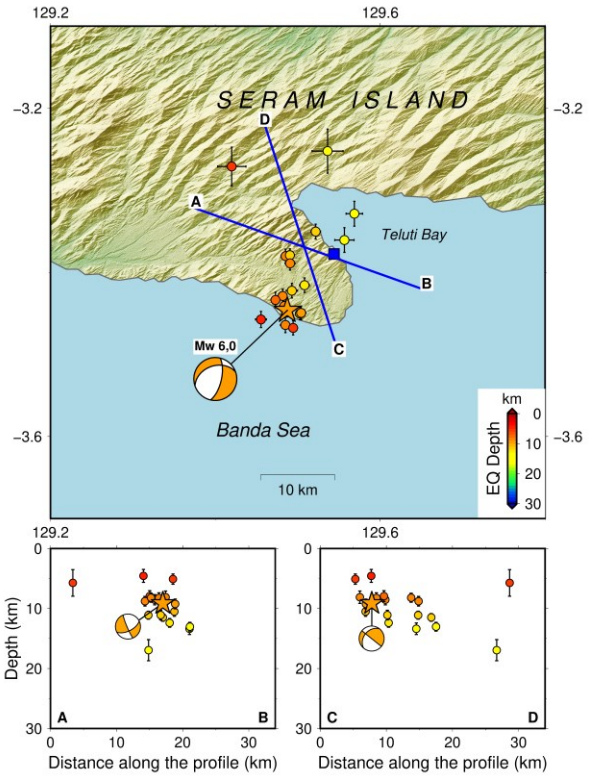

Fig. 7. Hypocenter distribution and vertical section after relocation for the mainshock (star) and the aftershocks (circles). Earthquakes depth is indicated by the color scale. Blue lines denote the cross-section profile perpendicular to the strike 13° fault plane (A-B) and strike 252° fault plane (C-D). Hypocenter location uncertainty after the relocation denoted by the error bars.

An important feature of the relocation results is the earthquake lineation shown in vertical cross-section of both the A-B profile perpendicular to strike 13° and the C-D profile perpendicular to strike 252°. The hypocenter lineation in A-B profile gives a tighter cluster of earthquakes with a dip angle of ~45° to the southeast direction (Figure 7). This is because the epicenter location has a northeast-southwest trending which is consistent with the strike direction. On the other hand, C-D profile shows earthquake location that are more scattered. Based on an empirical formula [15], a normal fault with Mw 6.0 will only have a rupture length of ~15 km and a downdip width of ~12 km. By using this calculation, we can interpret a gentler dip angle of ~35° facing to northwest direction (Figure 7). However, the earthquake distribution is not quite consistent with strike 252° horizontally.

We use geodetic observations to add constraints to the analysis. Station CBEM, one of stations from the Global Navigation Satellite System/Continuous Operating Reference Station (GNSS/CORS) network operated by the Geospatial Information Agency of Indonesia (BIG) that is located ~10 km toward northeast from the mainshock epicenter, has recorded a 14 mm northwest surface displacement (azimuth of 321°) and a 14 mm land subsidence (Figure 8). This ground deformation can be very well explained by the mechanism of the northwest-dipping fault plane (252° strike direction). Based on the relocated epicenter, the CBEM station is located on the hanging block of the fault which was experiencing downwards and northwestward slip displacement. This southwest-northeast oriented fault is also in accordance with the high-angle normal fault model which is thought to have formed due to near north-south extension activity in the central part of Seram Island. [4].

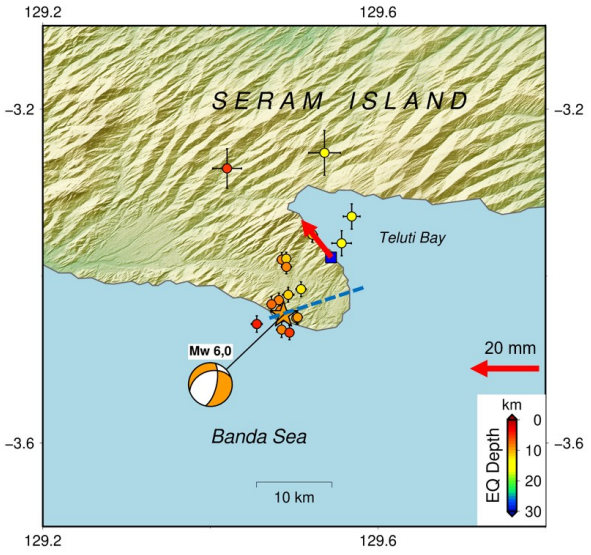

Fig. 8. Map showing the hypocenter location result from this study along with the estimated fault line (dashed blue line). A 14 mm horizontal displacement from CBEM CORS station (blue square) shown by red arrow.

Our results show that the hypocenter distribution does not correlate well with the fault structure. It is not impossible to assume that most of the aftershocks occurred along the downdip so it cannot accurately delineate the fault strike direction horizontally and the aftershocks that spread outside the main fault zone are considered as off-fault aftershocks. However, the imperfect azimuthal coverage of seismic stations should still be taken into consideration in the process of determining earthquake locations to avoid interpretation errors.

5 Conclusion

Relocation on the mainshock and aftershock sequence of the 2021 Mw 6.0 Tehoru earthquake has been carried out. The aftershocks distributed downward along a ~35° northwest-dipping plane which indicates a southwest-northeast fault orientation. This result confirmed by using geodetic observations that shows a horizontal displacement of 14 mm toward northwest direction and a land subsidence of 14 mm. We estimate that this earthquake sequence was caused by high-angle normal fault structure in Tehoru subdistrict and Teluti Bay area. This further confirms the north-south extension activity in the central part of Seram Island and the existence of another earthquake source on Seram Island apart from the Seram Trench and the Kawa Fault.

References

1. M. Heidarzadeh, A.R. Gusman, A. Patria, B.T. Widyantoro, Bul. Seis. Soc. Am. **112**, 2487 (2022)
2. J.M. Pownall, M.A. Forster, R. Hall, I.M Watkinson, Gond. Res. **44**, 35 (2017)
3. A. Patria, R. Hall, *The Origin And Significance Of The Seram Through, Indonesia*, in Proceedings of Indonesian Petroleum Association, IPA, May 2017, Jakarta, Indonesia (2017)
4. J.M. Pownall, R. Hall, I.M. Watkinson, Sol. Earth, **4**, 2 (2013)
5. P.A. Teas, J. Decker, D. Orange, P. Baillie, *New Insight Into Structure And Tectonics Of The Seram Through From Seaseep High Resolution Bathymetry*, in Proceedings of Indonesian Petroleum Association, IPA, May 2009, Jakarta, Indonesia (2009)
6. R. Hall, A. Patria, R. Adhitama, J.M. Pownall, L.T. White, *Seram, The Seram Through, The Aru Through, The Tanimbar Through And The Weber Deep: A New Look At Major Structures In The Eastern Banda Arc*, in Proceedings of Indonesian Petroleum Association, IPA, May 2017, Jakarta, Indonesia (2017)
7. A. Patria, H. Tsutsumi, D.H. Natawidjaja, J. Asian. Ear. Sci. **218**, 104881 (2021)
8. B. Sapiie, M. Hadiana, M. Patria, A.C. Adyagharini, A. Saputra, P. Teas, Widodo, *3D Structural Geology Analysis Using Integrated Analogue Sandbox Modeling : A Case Study Of The Seram Thrust-Fold Belt*, in Proceedings of Indonesian Petroleum Association, IPA, May 2012, Jakarta, Indonesia (2012)

9. F. Waldhauser, W.L. Ellsworth, Bul. Sei. Soc. Am. **90**, 1353 (2000)
10. F. Waldhauser, hypoDD: a computer program to compute double-difference hypocenter locations (U.S. Geol. Surv. Open File Rept., 2001)
11. G. Daniarsyad, D. Sianipar, N. Heryandoko, P. Priyobudi, Pure. Appl. Geo. **178** (2021)
12. D.P. Sahara, et al, Tectonophysics **799** (2021)
13. A.P. Cahyaningrum, A.D. Nugraha, N.T. Puspito, AIP. Proc. Conf., **1658** (2015)
14. B.L.N. Kennett, E.R. Engdahl, R. Buland, Geo. J. Int. **122**, 108 (1995)
15. K.K.S. Thingbaijam, P.M. Mai, K. Goda, Bul. Sei. Soc. Am. **107**, 2225 (2017)